Cosmological Implications of Fast Radio Burst Observations

Jatin Chowdhury[1]

[1] *Center for Computer Research in Music and Acoustics (CCRMA)*
Stanford University
660 Lomita Ct.
Stanford, CA 94305, USA

ABSTRACT

We present a general discussion of Fast Radio Bursts (FRBs), and the potential cosmological knowledge that can be gained from observations of FRBs. We include a discussion of measuring dispersion and scattering along the line-of-sight for an observed FRB, and show how to use FRBs as a probe to locate baryons. We also discuss using strongly lensed observations of FRBs to study dark matter, the Hubble Constant, and cosmic curvature. For each of the above discussions, we use simulated FRB observation data to show example calculations. At present, it appears that the primary cosmological contribution of FRBs will be their use in probing baryons and dark matter, as well as providing independent methods for measuring the Hubble Constant and cosmic curvature.

1. INTRODUCTION

Fast Radio Bursts (FRBs) are a relatively new astrophysical phenomenon, first observed in 2007 (Lorimer et al. 2007), consisting of brief (on the order of a millisecond) bursts of radio frequency radiation. While none of the many theories regarding the progenitors of FRBs has yet been proven correct (Platts et al. 2019), it is known that they are caused by a high-energy process, that some have been observed to repeat (Amiri et al. 2019), and that none have yet been observed within our own galaxy. As of this writing, just over 100 FRBs have been detected[1] (Petroff et al. 2016). With instruments like CHIME, ASKAP, the DSA, and UTMOST beginning to detect FRBs over the past couple of years, and new instruments such as HIRAX and the SKA expected to come online in the near future, it is expected that the number of detected FRBs will grow exponentially in the coming decade. A full list of instruments that have detected FRBs or are expected to detect FRBs is shown in fig. 1.

With more FRB detections expected, is worth examining some of the important cosmological information that can be extracted from these observations. While this writing only examines a couple of the possible ways that FRB observations can be used for cosmology, a brief yet comprehensive overview of FRB cosmology can be found in Weltman & Walters (2019).

The structure of this essay will be as follows: §2 will discuss the property of frequency dispersion as it effects FRB observations; §3 will discuss the effects of scattering on FRB observations; §4 will show how the dispersion characteristics of an FRB observation can be used to locate "missing" baryons; §5 will show how strongly-lensed observations of FRBs can be used to probe cosmological properties.

2. DISPERSION

As a photon from a Fast Radio Burst travels through the intergalactic medium (IGM), the photon experiences a frequency-dependent time delay due to its interactions with the free electrons in its path. The time delay is described by:

$$\Delta t = 4.2\nu_{\text{GHz}}^{-2}\left(\frac{DM}{10^3\text{cm}^{-3}\text{pc}}\right)\text{s} \tag{1}$$

[1] for an up-to-date list, see http://frbcat.org/

Telescope	Location	Operating Since	Number FRBs
Parkes Radio Telescope	Parkes, Australia	1963	27
Green Bank Telescope (GBT)	Green Bank, West Virginia, USA	2001	1
Arecibo Observatory	Arecibo, Puerto Rico	1963	2
Pushchino Radio Astronomy Observatory	Pushchino-on-Oka, Russia	1973	3
Molonglo Observatory Synthesis Telescope (UTMOST)	New South Wales, Australia	2015	3
Australian Square Kilometre Array Pathfinder (ASKAP)	Western Australia, Australia	2012	28
Canadian Hydrogen Intensity Mapping Experiment (CHIME)	Penticton, British Columbia, Canada	2017	21
Deep Synoptic Array 10-dish Prototype (DSA-10)	Owens Valley, California, USA	2019	1
Hydrogen Intensity and Real-time Analysis eXperiment (HIRAX)	Karoo, South Africa	2021 (projected)	N/A
Square Kilometre Array (SKA)	Australia, South Africa	2027 (projected)	N/A

Figure 1. A list of telescopes that have detected or are expected to detect Fast Radio Bursts.

where ν is the frequency of the photon. The "dispersion measure" DM is defined as (McQuinn 2014):

$$DM(z_s) = \int_0^{z_s} \frac{n_e(z)}{1+z} dz \tag{2}$$

where z_s is the redshift of the source to the observer, and n_e is the electron density at a certain point along the line-of-sight, a redshift z from the observer. In practice, the dispersion measure of an FRB is typically estimated during the detection of the FRB; then using a model of free electron density, (see, e.g. Yao et al. (2017)), astronomers are able to estimate the distance at which the FRB originated (CHIME/FRB Collaboration et al 2018).

Note that while the host galaxy of the FRB as well as our own galaxy contribute somewhat to the dispersion measure, for bursts occuring at cosmological scales the dispersion caused by the IGM is dominant.

2.1. *Simulation*

We can now examine the process of FRB dispersion through simulation. We fist generate an simulated burst with pulse width 0.05 milliseconds and signal-to-noise ratio of 10 in the 1-2 GHz band (fig. 3). Using a high-order allpass filter, we can simulate the dispersion characteristic described by eq. (7) with the process described in Abel & Smith (2006). In this example, we use a dispersion measure of 250 pc cm^{-3}. The resulting burst profile and frequency spectrum can be seen in fig. 4.

3. SCATTERING

Along with being dispersed, the light from a Fast Radio Burst is scattered by the particles it interacts with along its path, as evidenced by the broadened pulse width observed in FRBs. While some of the scattering can be accounted for by elements within our own Galaxy, the total intra-galactic scattering does not account for the total scattering observed from FRBs, indicating additional scattering from the FRB's host galaxy and/or the intergalactic medium.

The mechanism for this time scattering is the turbulence present in the IGM. In this writing, we assume the turbulence follows a Kolmogorov scaling, with outer scale L_0, and inner scale $l_0 << L_0$. The effective "scattering measure" due to the IGM can then be defined as (Zhu et al. 2018):

$$SM_{eff}(z_s) = \int_0^{z_s} \frac{C_N^2(z) d_H(z)}{(1+z)^3} dz \tag{3}$$

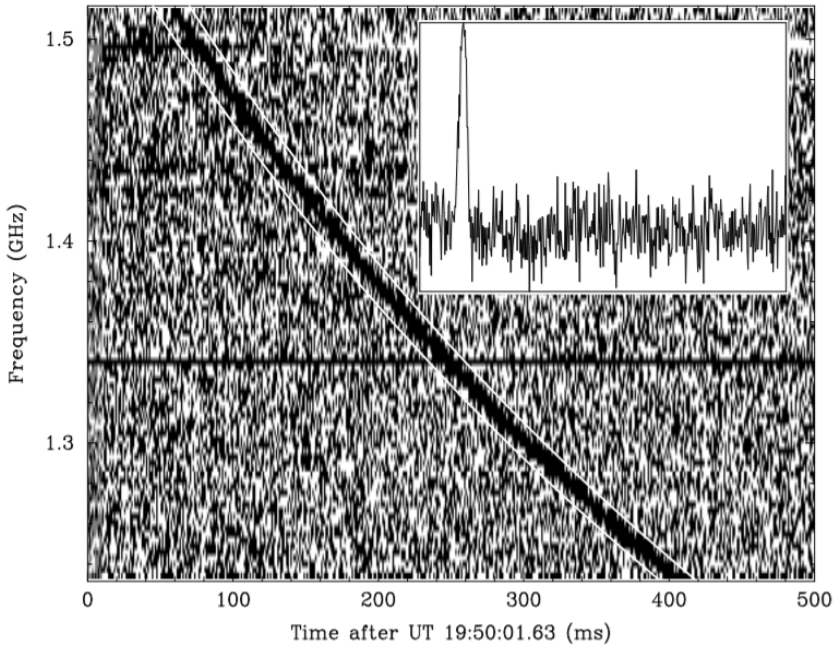

Figure 2. A "waterfall" plot of the first observed Fast Radio Burst. Note the dispersion of the burst, as evident by the fact that the high frequencies arrive prior to the lower frequencies. Reproduced from Lorimer et al. (2007).

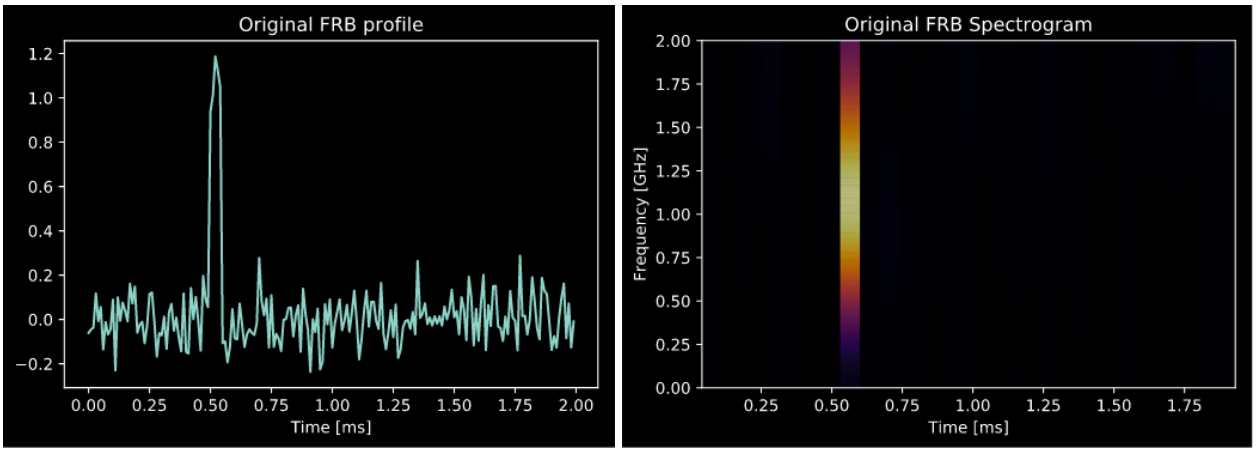

Figure 3. *A time series plot (left), and a spectrogram (right) of an FRB before experiencing any dispersion or scattering.*

where $d_H(z) = cH_0^{-1}[\Omega_\Lambda + \Omega_m(1+z)^3]^{-1/2}$ is the Hubble radius. $C_N^2(z)$ is a factor related to the variance of the electron density $\langle \delta n_e^2(z) \rangle$, given as

$$C_N^2(z) \approx \frac{\beta - 3}{2(2\pi)^{4-\beta}} \langle \delta n_e^2(z) \rangle L_0^{3-\beta} \tag{4}$$

In this equation, the density power spectrum of the turbulence can be described by a power law with index $\beta > 3$, between the outer and inner scales.

4. FRBS AND THE MISSING BARYON PROBLEM

One of the reasons Fast Radio Bursts are particularly interesting to astronomers and cosmologists, is that they can potentially serve as probes to measure the baryonic content of the universe. Recent surveys of the nearby universe have only accounted for approximately half of the baryonic mass that we expect to find in the universe according both to modern cosmological theory, as well as measurements of hydrogen density in the intergalactic gas from 10 billion

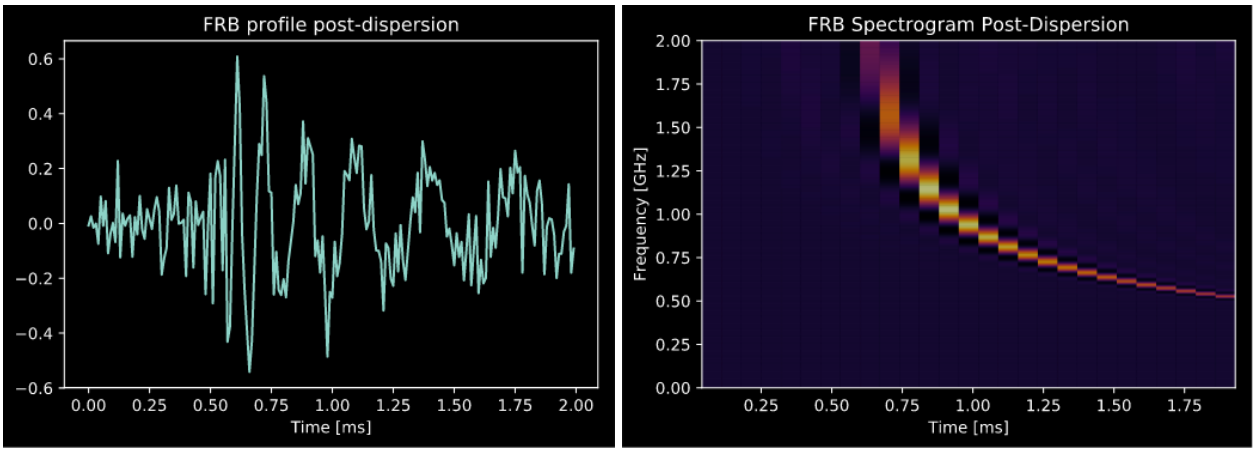

Figure 4. *A time series plot (left), and a spectrogram (right) of an FRB after experiencing dispersion.*

years ago (McQuinn 2014). FRBs are a uniquely fine-tuned probe for locating baryons since every ionized baryon along the line of sight contributes to the FRB's dispersion measure.

In practice, the baryonic matter density can be estimated from an FRB observation using the following equation, assuming all the baryons are located in the IGM (Macquart 2018):

$$DM = \frac{3cH_0\Omega_b}{8\pi G m_p}\int_0^z \frac{(1+z')f_{IGM}(\frac{3}{4}X_{e,H}(z')+\frac{1}{8}X_{e,He}(z'))}{\sqrt{\Omega_m(1+z')^3+\Omega_\Lambda f(z',w)}}dz' \tag{5}$$

This equation assumes a flat universe, with Ω_b, Ω_m, and Ω_Λ denoting the densities of baryons, matter, and dark energy in the universe, respectively. $X_{e,H}$ and $X_{e,He}$ describe the ionization fractions of hydrogen and helium, f_{IGM} is the fraction of all baryons that exist in the IGM.

Macquart (2018) points out that for FRBs to be a useful probe of baryonic matter, it is necessary for the FRBs to be localised to a host galaxy, both to determine the host galaxy redshift z needed for eq. (5), as well as to remove the DM contribution from the host galaxy.

4.1. *Example Calculation*

As an example let us examine FRB 190523, an FRB detected in May of 2019 by the Deep Synoptic Array 10-dish prototype at the Owens Valley Radio Observatory. This FRB observation is notable for being the first non-repeating FRB to be localised to a host galaxy (Ravi et al. 2019). FRB 190523 has a dispersion measure of 750 pc cm^{-3}, and was localised to a host galaxy with redshift $z = 0.66$. For this example calculation, we use cosmological parameters as determined by the most recent Planck survey: $H_0 \approx 68$ km s^{-1} Mpc^{-1}, $\Omega_\Lambda = 0.69$, $\Omega_m = 0.31$ (Planck Collaboration et al 2018). We assume full ionization of hydrogen and helium ($X_{e,H} = 1$, $X_{e,He} = 1$), $f(z', w) = 1$, and use $f_{IGM} = 0.8$, as approximated by Li et al. (2019). With these values, we see eq. (5) as:

$$750\frac{\text{pc}}{\text{cm}^3} = \frac{3\left(3\times10^8\frac{\text{m}}{\text{s}}\right)\left(68\frac{\text{km}}{\text{s Mpc}}\right)\Omega_b}{8\pi\left(6.67\times10^{-11}\frac{\text{m}^3}{\text{kg s}^2}\right)(1.67\times10^{-27}\text{kg})}\int_0^{0.66}\frac{(1+z')(0.8)(\frac{3}{4}+\frac{1}{8})}{\sqrt{(0.31)(1+z')^3+(0.69)}}dz' \tag{6}$$

After carrying out the integral and simplifying the units, we find $\Omega_b = 0.065$. This result is of the same order of magnitude as the latest estimation from the Planck survey ($\Omega_b \approx 0.049$), and can be improved with more well-informed estimates of parameters including f_{IGM}, $X_{e,H}$, and $X_{e,He}$. The above calculation can be repeated for more FRBs as they are discovered and localised to their host galaxies, helping to average out systematic errors and giving us a more precise estimate of how much of the missing baryonic matter is located in the IGM thereby contributing to the dispersion of these FRBs.

5. FAST RADIO BURSTS AND STRONG LENSING

Along with the properties of the universe that can be measured through the analysis of FRB dispersion and scattering, it is possible that with lensed observations of FRBs we may have additional methods for probing dark matter, cosmic curvature, and the Hubble constant.

From a practical standpoint, obtaining strongly lensed FRB observations may seem unlikely, given the inherently unpredictable nature of FRBs. Li et al. (2018) give some thoughts on this issue, noting that with HIRAX, UTMOST, CHIME, and the SKA all online we can expect to observe more than 100 FRBs per day (Fialkov & Loeb 2017), and that the probability for an FRB with $z > 1$ to be strongly lensed is on the order of 10^{-4} (Hilbert et al. 2008). Combining these predictions with knowledge that some FRBs have been observed to repeat (Spitler et al. 2016; Amiri et al. 2019), Li et al. (2018) predicts we will have observed ~ 10 strongly lensed FRBs within 30 years from when the SKA begins operation.

One of the reasons that FRBs are a good candidate for strong lensing analysis in particular is that there is a large disparity between the short length of an FRB $\sim \mathcal{O}$ (ms) and the much longer length of a typical galaxy-lense delay time $\sim \mathcal{O}$ (10 days). This disparity allows for great precision in calculating the delay time of the lense. Further, for the first repeating FRB (121102), we have been able to obtain accurate localizations, and high-resolution images of their FRB's host galaxy, using deep observations from the VLA (Tendulkar et al. 2017). For a strongly lensed FRB, these follow-up observations will allow us to model the mass profile of the lense with high precision.

From lensing theory, we can express the time delay between two lensed images A and B as (Kochanek & Schechter 2003):

$$\Delta\tau_{AB} = \frac{\Delta\Phi_{AB}}{c}(1+z_l)\frac{D_l^A D_s^A}{D_{ls}^A} \tag{7}$$

where z_l is the redshift of the lense, and the D terms represent the angular diameter distances from observer to lens (D_l^A), observer to source (D_s^A), and lens to source (D_{ls}^A). $\Delta\Phi_{AB}$ is the Fermat potential difference between the two image positions.

5.1. *Hubble Constant*

It is common to define the "time-delay distance" $D_{\Delta t}$ as

$$D_{\Delta t} = (1+z_l)\frac{D_l^A D_s^A}{D_{ls}^A} \tag{8}$$

$D_{\Delta t}$ has units of distance and is inversely proportional to the Hubble Constant. Again, because of the disparity between the time scales of Fast Radio Bursts and lense-delay times, the delay time uncertainty is virtually negligible. Due to this increased precision, Li et al. (2018) predict that with ~ 10 observations of lensed FRBs, the Hubble Constant can be measured with an uncertainty of $\sim 0.91\%$. This precision gives a factor of ~ 5 improvement over Hubble Constant measurements from observations of multiply-lensed quasars (e.g., Suyu et al. (2017)). This improvement is due primarily to having a much higher precision measurement of the time delay $\Delta\tau_{AB}$.

FRB measurements of the Hubble Constant are important due to the current tension between measurements made by CMB observations (e.g. Planck), and measurements made from observing standard candles (Cepheid variables, type 1a supernovae) and using a distance-ladder approach. Strong-lensing measurements of H_0 are nice because they come with an independent set of underlying assumptions, and because the measurements can be easily applied to a variety of cosmological models (Suyu et al. 2017). With the potential improvements that strongly-lensed FRB observations may provided over quasars, it will be interesting to see how such experiments play out, though actual lensed FRB observations have yet to be found.

5.2. *Cosmic Curvature*

From the properties used to calculate the time-delay distance, it is also relatively straightforward to measure cosmic curvature. Simply, we can construct dimensionless comoving angular diameter distances:

$$\begin{aligned} d_l &= (1+z_l)\frac{H_0 D_l^A}{c} \\ d_s &= (1+z_s)\frac{H_0 D_s^A}{c} \\ d_{ls} &= (1+z_s)\frac{H_0 D_{ls}^A}{c} \end{aligned} \tag{9}$$

where z_s is the redshift of the source. From these values, we can say that if d_s is greater than, equal to, or smaller than $d_l + d_{ls}$, then the geometry of space is open, flat, or closed, respectively. With that in mind, Li et al. (2018) propose combining time-delay distance measurements with measurements of distances from type 1a supernovae to directly measure spatial curvature, independent of any assumed cosmological model.

Specifically, Li et al. (2018) propose using a distance sum rule (Peebles 1993), where

$$d_{ls} = d_s\sqrt{1+\Omega_k d_l^2} - d_l\sqrt{1+\Omega_k d_s^2} \tag{10}$$

and Ω_k denotes cosmic curvature. To best compare with a time-delay distance measurement as described by eq. (8), the distance sum rule can be re-arranged as (Liao et al. 2017):

$$\frac{d_{ls}}{d_l d_s} = \frac{1}{d_l}\sqrt{1+\Omega_k d_l^2} - \frac{1}{d_s}\sqrt{1+\Omega_k d_s^2} \tag{11}$$

Again, the advantage of using FRBs for this calculation is that the uncertainty in the measured time delay is effectively zero, due to brief length of an FRB relative to the length of a typical galaxy lense delay. Therefore the only uncertainties in estimating cosmic curvature from FRB time delays come from the uncertainty in Fermat potential difference $\Delta\Phi_{AB}$, and line-of-sight contamination. Assuming an uncertainty in the Fermat potential difference $\delta\Delta\Phi_{AB} = 0.8\%$ and uncertainty due to line-of-sight contamination $\delta\kappa_{\rm ext} = 2\%$, Li et al. (2018) use simulated FRB data to predict that with ~ 10 observations of lensed FRBs, the value of cosmic curvature can be estimated with a precision of ~ 0.076.

5.3. *Dark Matter*

The possibility of using strongly lensed observations of FRBs to locate dark matter is discussed by Muñoz et al. (2016). While cosmologists have deducted from observations that much of the matter density of the universe is made up of dark matter, a significant portion of this dark matter is yet unaccounted for. One potential candidate for dark matter is the so-called "massive compact halo object" (MACHO). The number of compact objects made of dark matter that can exist in MACHOs larger than 100 $M_\odot$ and smaller than 20 $M_\odot$ has been tightly constrained, but it is possible that a large quantity of compact objects in the intermediate range could be MACHOs.

If an FRB were to be strongly lensed by a MACHO with mass $M_L \sim 20 - 100\ M_\odot$, the resulting time-delay would be on the order of milliseconds, and for an FRB with sufficiently short pulse width, the time delay would cause a "double-peaked" FRB signal to be detected from telescopes on Earth. Muñoz et al. (2016) claims that if all the missing dark matter resides in MACHOs, approximately one in every fifty FRBs occuring at redshift $z = 0.5$ will be lensed in this fashion.

By treating a MACHO with mass M_L as a point lens with an Einstein angular radius

$$\theta_E = 2\sqrt{\frac{GM_L}{c^2}\frac{D_{ls}^A}{D_l^A D_s^A}} \tag{12}$$

The images produced by the lense will occur at positions $\theta_\pm = (\beta \pm \sqrt{\beta^2 + 4\theta_E^2})/2$, where β is the angular impact parameter. Then the time delay equation eq. (7) can be written as:

$$\Delta\tau_{A,B} = \frac{4GM_L}{c^3}(1+z_l)\left[\frac{y}{2}\sqrt{y^2+4} + \log\left(\frac{\sqrt{y^2+4}+y}{\sqrt{y^2+4}-y}\right)\right] \tag{13}$$

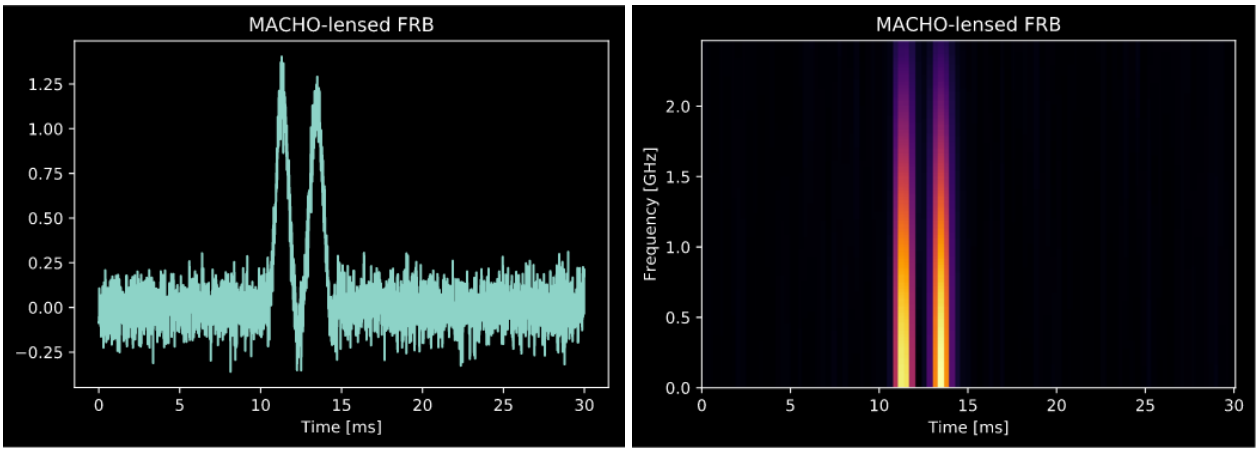

Figure 5. *A time series plot (left), and a spectrogram (right) of an FRB lensed by a MACHO with mass* $M_L = 80\ M_\odot$.

for normalized impact parameter $y \triangleq \beta/\theta_E$. From this equation, with a measured time delay, it is possible to estimate the mass of the MACHO.

5.3.1. *Example Calculation*

As an example of this phenomonen, we have generated a simulated FRB at redshift $z = 0.66$ and pulse width of 1 millisecond, and a simulated MACHO lens with mass $M_L = 80\ M_\odot$, and redshift $z = 0.33$. Assuming a flat ΛCDM cosmology, and using the latest cosmological parameters from the Planck survey, as in §4.1, the expected time delay is 2.12 milliseconds. The resulting "doubly peaked" FRB observation is shown in fig. 5, assuming the observation has already had dispersion, scattering, and other such effects removed. Note that for FRBs with larger pulse widths, it may not be possible to distinguish the separate peaks caused by the MACHO lens.

If "doubly peaked" FRBs of this sort are observed, it will allow us to locate a potentially significant amount of the missing dark matter in the universe today. Conversely, if no MACHO-lensed FRBs are found, we will be able to place strong constraints on the fraction of dark matter f_{DM} that may reside in MACHOs. Muñoz et al. (2016) constrain $f_{DM} \lesssim 0.08$ for $M_L \gtrsim 20\ M_\odot$, if no MACHO-lensed FRBs are found.

6. CONCLUSION

In this writing, we have given a brief discussion of Fast Radio Bursts, noting their recent observations and unknown origins. We have examined the effects of dispersion and scattering on FRBs travelling through the IGM, and attempted to use the Dispersion Measure of a recently observed FRB (190523) to estimate the density of baryonic matter. Finally, we have explored the possibilities of using strongly-lensed FRB observations to probe dark matter, cosmic curvature, and the Hubble Constant.

With potentially thousands of FRB detections per year on the horizon, and new instruments including CHIME, HIRAX, and the SKA either recently, or soon-to-be coming online, it is an exciting time to think about the cosmological implications of FRB observations. With the impending influx of data, it is hoped that the methods and possibilities discussed in this writing will be improved upon and brought to fruition in the near future, adding new knowledge to our understanding of the cosmological universe.

REFERENCES

Abel, J. S., & Smith, J. O. 2006, Proc. of the 9th Int. Conference on Digital Audio Effects. https://pdfs.semanticscholar.org/3978/5c4d9aaf34d181b568a922c6654da234548e.pdf

Amiri, M., Bandura, K., Bhardwaj, M., et al. 2019, Nature, 566, 235, doi: 10.1038/s41586-018-0864-x

CHIME/FRB Collaboration et al. 2018, The Astrophysical Journal, 863, doi: https://doi.org/10.3847/1538-4357/aad188

Fialkov, A., & Loeb, A. 2017, The Astrophysical Journal, 846, L27, doi: 10.3847/2041-8213/aa8905

Hilbert, S., White, S. D. M., Hartlap, J., & Schneider, P. 2008, Monthly Notices of the Royal Astronomical Society, 386, 1845–1854, doi: 10.1111/j.1365-2966.2008.13190.x

Kochanek, C. S., & Schechter, P. L. 2003. https://arxiv.org/abs/astro-ph/0306040

Li, Z., Gao, H., Wei, J.-J., et al. 2019, The Astrophysical Journal, 876, 146, doi: 10.3847/1538-4357/ab18fe

Li, Z.-X., Gao, H., Ding, X.-H., Wang, G.-J., & Zhang, B. 2018, Nature Communications, 9, 3833, doi: 10.1038/s41467-018-06303-0

Liao, K., Li, Z., Wang, G.-J., & Fan, X.-L. 2017, The Astrophysical Journal, 839, 70, doi: 10.3847/1538-4357/aa697e

Lorimer, D. R., Bailes, M., McLaughlin, M. A., Narkevic, D. J., & Crawford, F. 2007, Science, 318, 777, doi: 10.1126/science.1147532

Macquart, J.-P. 2018, Probing the Universe's baryons with fast radio bursts. https://arxiv.org/abs/1811.00197

McQuinn, M. 2014, The Astrophysical Journal Letters, 780, doi: https://doi.org/10.1088/2041-8205/780/2/L33

Muñoz, J. B., Kovetz, E. D., Dai, L., & Kamionkowski, M. 2016, Physical Review Letters, 117, doi: 10.1103/physrevlett.117.091301

Peebles, P. J. E. 1993, Principles of physical cosmology (Princeton University Press)

Petroff, E., Barr, E. D., Jameson, A., et al. 2016, PASA, 33, e045, doi: 10.1017/pasa.2016.35

Planck Collaboration et al. 2018, Planck 2018 results. VI. Cosmological parameters

Platts, E., Weltman, A., Walters, A., et al. 2019, Physics Reports, 821, 1 , doi: https://doi.org/10.1016/j.physrep.2019.06.003

Ravi, V., Catha, M., D'Addario, L., et al. 2019, Nature, 572, 352, doi: doi:10.1038/s41586-019-1389-7

Spitler, L., Scholz, P., Hessels, J., et al. 2016, Nature, 531, 202, doi: https://doi.org/10.1038/nature17168

Suyu, S. H., Bonvin, V., Courbin, F., et al. 2017, Monthly Notices of the Royal Astronomical Society, 468, 2590–2604, doi: 10.1093/mnras/stx483

Tendulkar, S. P., Bassa, C. G., Cordes, J. M., et al. 2017, The Astrophysical Journal, 834, L7, doi: 10.3847/2041-8213/834/2/l7

Weltman, A., & Walters, A. 2019

Yao, J., et al. 2017, The Astrophysical Journal, 835, doi: https://doi.org/10.3847/1538-4357/835/1/29

Zhu, W., Feng, L.-L., & Zhang, F. 2018, The Astrophysical Journal, 865, 147, doi: 10.3847/1538-4357/aadbb0